

1 Abstract

## 2 **Purpose/Objectives**

3 To evaluate the use of diffusion-weighted magnetic resonance imaging  
4 (DW-MRI) and  $^{18}\text{F}$ -fluorodeoxyglucose (FDG) positron emission tomography (PET) for  
5 predicting disease progression (DP) among patients with non-small cell lung carcinoma  
6 (NSCLC) treated with stereotactic body radiotherapy (SBRT).

7

## 8 **Materials/Methods**

9 Fifteen patients with histologically confirmed stage I NSCLC who underwent  
10 pre-treatment DW-MRI and PET and were treated with SBRT were enrolled. The mean  
11 apparent diffusion coefficient (ADC) value and maximum standardised uptake value  
12 ( $\text{SUV}_{\text{max}}$ ) were measured at the target lesion and evaluated for correlations with DP.

13

## 14 **Results**

15 The median pre-treatment ADC value was  $1.04 \times 10^{-3}$  (range  $0.83\text{--}1.29 \times 10^{-3}$ )  
16  $\text{mm}^2/\text{s}$ , and the median pre-treatment  $\text{SUV}_{\text{max}}$  was 9.9 (range 1.6–30). There was no  
17 correlation between the ADC value and  $\text{SUV}_{\text{max}}$ . The group with the lower ADC value ( $\leq$   
18  $1.05 \times 10^{-3} \text{ mm}^2/\text{s}$ ) and that with a higher  $\text{SUV}_{\text{max}}$  ( $\geq 7.9$ ) tended to have poor DP, but  
19 neither trend was statistically significant ( $p = 0.09$  and  $0.32$ , respectively). The

20 combination of the ADC value and  $SUV_{max}$  was a statistically significant predictor of DP  
21 ( $p = 0.036$ ).

22

### 23 **Conclusion**

24 A low ADC value on pre-treatment DW-MRI and a high  $SUV_{max}$  may be  
25 associated with poor DP in NSCLC patients treated with SBRT. Using both values in  
26 combination was a better predictor.

27 **Introduction**

28 Surgery is widely accepted as a standard therapy for stage I non-small cell lung  
29 cancer (NSCLC); however, some patients with stage I NSCLC are not suited for resection  
30 mainly because of their poor respiratory function.

31 Stereotactic body radiotherapy (SBRT) has recently been accepted as an  
32 alternative therapy for patients with stage I NSCLC who cannot undergo surgery or  
33 decline surgery [1-3]. In a previous study, medically inoperable patients were treated with  
34 peripheral T1-T2N0M0 NSCLC using SBRT [4]; the authors reported 3-year local control  
35 rates of 97.6% in a group of 55 patients with a median follow-up of almost 3 years, but  
36 distant metastasis was 22.1%. We previously reported a 3-year local control rate of 86.8%  
37 and a progression-free rate of 59.2% [5].

38 Histological findings are important factors for the determination of a treatment  
39 strategy and to predict clinical outcomes [6]. In lung SBRT, pathological diagnosis is  
40 confirmed in most patients before treatment is administered, however some patients  
41 undergo the treatment without histological confirmation due to the risk of adverse events  
42 caused by biopsy. Simple and less-invasive alternative methods are needed to stratify  
43 patients according to risk of disease progression (DP).

44 Advances in imaging technologies such as diffusion-weighted magnetic resonance  
45 imaging (DW-MRI) and <sup>18</sup>F-fluorodeoxyglucose (FDG) positron emission tomography  
46 (PET) have made it possible to evaluate not only morphological aspects, but also

47 functional aspects including diffusion motion of water molecules and glucose metabolism  
48 in tumours. These recently developed imaging techniques are applied to improve the  
49 sensitivity of tumour detection and prediction accuracy of the clinical outcomes. Several  
50 studies have analysed the utility of FDG-PET for the prognosis and prediction of  
51 therapeutic effect after treatment of NSCLC [7-9]. The apparent diffusion coefficient  
52 (ADC) of a tumour based on DW-MRI has been reported to be a useful indicator for early  
53 prediction of tumour response and prognosis in other cancers treated with  
54 chemoradiotherapy [10, 11]. To date, no study has evaluated the use of DW-MRI as a  
55 predictor for NSCLC treated with SBRT. Several studies have found that PET might be a  
56 useful predictor for patients with early-stage NSCLC treated with SBRT, but the results  
57 are controversial [12-15].

58         In this study, we evaluated whether pre-treatment DW-MRI and PET could be  
59 used to predict the clinical outcome of stage I NSCLC outcomes after SBRT and  
60 compared their predictive capabilities in the same tumours.

61

## 62 **Materials/Methods**

### 63 **Subjects**

64         The eligibility criteria for lung SBRT in our hospital were as follows: (1)  
65 T1a-T2aN0M0 lung tumour, (2) inoperable or refusal to undergo surgery, (3) arms could  
66 be held over the head for 30 min or more, and (4) performance status of 0–2.

67           Fifteen patients with histologically confirmed NSCLC who underwent  
68 pre-treatment DW-MRI and FDG-PET and were treated with SBRT in our hospital  
69 between January and December of 2010 were included this study. This study was  
70 approved by our Institutional Review Board. The median age was 80 years (range, 70–86  
71 years). Eleven patients were male and four were female. Patients were staged according to  
72 the Union for International Cancer Control's TNM classification, 7<sup>th</sup> edition with CT and  
73 FDG-PET. Contrast medium was administered in the CT scan, if possible. The mean  
74 diameter of the tumours was 28 mm (range, 14–42 mm). T stages were distributed as  
75 follows: T1a in four, T1b in six, and T2a in five patients. Histological examinations  
76 included transbronchial biopsy (10 patients) or percutaneous CT-guided biopsy (5  
77 patients) and were conducted before the pre-treatment DW-MRI and FDG-PET. The  
78 median interval between the biopsy and these imaging was 43 days (range, 17–67 days).  
79 The detailed characteristics of all patients are shown in Table 1.

80

81 SBRT procedure

82           The details of the SBRT procedure were described previously [16]. The patient's  
83 body was immobilised with an individualised vacuum pillow (BodyFIX; Elekta AB,  
84 Stockholm, Sweden). The SBRT protocol was created with a commercial treatment  
85 planning system, iPlan (BrainLab, Feldkirchen Germany). Four-dimensional computed  
86 tomography (4DCT) data were acquired in axial cine mode using a 16-slice CT scanner

87 (LightSpeed RT16, GE Healthcare, Waukesha, WI, USA) and real-time positioning  
88 management system (Varian Medical Systems, Palo Alto, CA, USA). An internal target  
89 volume (ITV) was determined by assessing tumour trajectory using 4DCT and tumour  
90 motion by X-ray fluoroscopy. Both techniques were employed because 4DCT is only  
91 capable of evaluating one respiratory cycle, and X-ray fluoroscopy can be used to evaluate  
92 the changes of tumour motion amplitude and duration of the respiratory cycle in several  
93 respiratory cycles. Planning target volume (PTV) was defined as ITV + margin (5mm).

94       Irradiation was performed with 6 MV X-ray beams from a linear accelerator  
95 (Novalis BrainLab) in multiple coplanar and noncoplanar static ports (6 to 8 ports). The  
96 dose was prescribed to the isocentre and dose distribution in PTV was homogeneous. The  
97 70%-80% isodose lines encompassed the PTV edge. Dose distribution was calculated  
98 with the X-ray Voxel Monte Carlo method.

99       Prescribed doses and fractions were 48 Gy/4 fr (biologically effective dose [BED]  
100 of 105.6 Gy<sub>10</sub>) for T1a-T1b, 56 Gy/4 fr (BED 134.0 Gy<sub>10</sub>) for T2a, and 60 Gy/8 fr (BED  
101 105.0 Gy<sub>10</sub>) for centrally located tumours within 2 cm of the trachea or proximal bronchial  
102 tree, great vessels, and other mediastinal structures, regardless of their size. Overall  
103 treatment time was 4 to 11 days.

104

105 MRI protocol

106 All MRI examinations were performed using a 1.5T MR unit (Avanto, Siemens,  
107 Erlangen, Germany) with a phased-array coil. All patients were imaged in the supine  
108 position. Initially, transverse HASTE images were obtained for anatomical identification.  
109 Subsequently, both T2-weighted (TR/TE = 2100/85 ms) and DW-MR images with  
110 prospective acquisition correlation (PACE) utilising sensitivity encoding (SENSE; with a  
111 SENSE factor of 2) and echo planar imaging (EPI; with an EPI factor of 96) were  
112 obtained. The parameters used for DW-MRI were a TR/TE of 2746.3–12030.4/72–79 ms,  
113 FOV of 320 mm, slice thickness of 4.0 mm, matrix of  $96 \times 128$  mm, band width of 1860  
114 Hz/pixel and five excitations. All DW-MR images were acquired with MPG pulses in  
115 three directions (the x, y, and z axes) with three different b-factors (0, 500, and 1000  
116  $\text{s}/\text{mm}^2$ ). All MR images covered the entire chest. ADC maps were automatically  
117 calculated from a series of DW images according to a linear regression model based on  
118 the logarithm of signal intensities as follows:

$$119 \quad \text{ADC} = (\log \text{SI}_1/\text{SI}_0)/b$$

120 where  $\text{SI}_1$  is the signal intensity with a diffusion gradient,  $\text{SI}_0$  is the signal intensity  
121 without a diffusion gradient, and  $b$  is the gradient factor of sequences.

122 The ADC values of each tumour were measured by a single observer (SU) with 10  
123 years of experience in clinical chest MRI. The mean signal intensity of the tumour was  
124 measured on an ADC map within three different circular regions of interest (ROIs) that  
125 were as large as possible. The average of these was calculated as the ADC value of the

126 tumour. All ROIs were established in the centre of the tumour to avoid artefacts from the  
127 tumour/air interface or from blood flow in the surrounding large vessels. T2-weighted MR  
128 images were also used as a reference, to avoid inclusion of necrotic areas in the ROIs. The  
129 respiratory gating method was used for the MRI scan.

130

131 FDG-PET protocol

132 Patients fasted for at least 4 h before the examination, and their plasma glucose  
133 level was checked immediately before the administration of  $^{18}\text{F}$ -FDG ( $\sim 3.7$  MBq/kg). No  
134 patients had a plasma glucose level greater than 200 mg/dL. Approximately 1 h later,  
135 PET/CT was performed, using a combined PET/CT scanner (Discovery ST Elite, GE  
136 Healthcare Waukesha, WI, USA). Low-dose CT images were acquired during shallow  
137 breathing from the upper thigh to the skull base with a 16-detector row scanner (20–100  
138 mA, using the auto-mA setting with a noise index of 30, 120 kV, 0.6 s tube rotation, slice  
139 thickness 3.75 mm, matrix 512×512, and a pitch of 1.75). Immediately after CT, a  
140 whole-body PET emission scan was performed in 3D-acquisition mode with an  
141 acquisition time of 2–3 min per bed position. The PET images were attenuation-corrected  
142 using the CT data and were reconstructed with a 3D ordered-subsets expectation  
143 maximisation algorithm. The respiratory gating method was not used for the PET scan.  
144 The maximum standardised uptake values ( $\text{SUV}_{\text{max}}$ ) were measured at the target lesion by  
145 a single observer (YN) with more than 10 years of experience in nuclear medicine.

146

147 Follow-up

148 Follow-up visits were conducted at 1, 2, 3, 6, 9, and 12 months in the first year  
149 after SBRT and every 3–6 months thereafter. The plain CT scan was performed every 3  
150 months in the first year after treatment and every 3–6 months thereafter. When DP was  
151 highly suspected by the CT scan, FDG-PET was also performed.

152 Local progression (LP) was diagnosed based on the recommendations for  
153 follow-up imaging established by Huang et al. [17]. Regional lymph node metastases  
154 were diagnosed based on CT. FDG-PET results were also considered in diagnosis but  
155 histological confirmation was not mandatory. DP was defined as LP, regional lymph node  
156 metastases, or distant metastases.

157

158 Statistical analysis

159 The correlation of ADC value and  $SUV_{max}$  with DP after SBRT was evaluated. LP  
160 and overall survival (OS) were evaluated in the same manner. To consider the impact that  
161 the tumour diameter gives the ADC value and  $SUV_{max}$ , the correlations of ADC value and  
162  $SUV_{max}$  with tumour size were also evaluated. The cumulative incidence of DP and LP  
163 was evaluated considering competing risk of non-lung cancer death. The Kaplan–Meier  
164 method was used to estimate OS and the Grey-box test and log-rank test were used to  
165 detect differences between strata. A  $p$ -value  $< 0.05$  was considered statistically significant.

166 Receiver operating characteristic (ROC) analyses were performed to determine  
167 appropriate thresholds of ADC value and  $SUV_{max}$ . All statistical analyses were performed  
168 with R software (version 2.15.1, R Development Core Team)[18].

169

## 170 **Results**

### 171 **Survival**

172 The median follow-up period was 28.0 (range, 6.7–37.2) months. DP was  
173 observed in nine patients. The first site of progression was local tumour in three patients,  
174 regional lymph node in two patients, and distant metastasis in four patients. Seven of the  
175 nine DP were diagnosed with CT and FDG-PET. The remaining two patients who  
176 developed lung metastases were diagnosed with plain CT.

177 The OS at 24 months was 52% (seven patients died, 95% confidence interval [CI],  
178 26–74%). The cumulative incidence rates of LP and DP were 16% (two patients) and 57%,  
179 (nine patients) respectively, at 24 months.

### 180 **ADC value and $SUV_{max}$**

181 The pre-treatment ADC values ranged from 0.83 to  $1.29 \times 10^{-3}$  mm<sup>2</sup>/s (median  
182  $1.04 \times 10^{-3}$  mm<sup>2</sup>/s), and  $SUV_{max}$  ranged from 1.5 to 30.0 (median 9.9). There was no  
183 statistically significant correlation between ADC value and  $SUV_{max}$  (Fig. 1). Fig. 2 shows  
184 the scatter plot of tumour diameter and ADC value and  $SUV_{max}$ . ADC value and  $SUV_{max}$   
185 showed weak positive correlations with tumour diameter with correlation coefficients of

186 0.48 and 0.50, but without statistical significance ( $p = 0.64$  and  $0.63$ , respectively).

187 According to the ROC analysis the appropriate threshold values for DP were  $1.05 \times 10^{-3}$   
188  $\text{mm}^2/\text{s}$  for ADC value and  $7.9$  for  $\text{SUV}_{\text{max}}$ .

189 When dividing the patients into two groups according to the threshold ADC value  
190 of  $1.05 \times 10^{-3} \text{mm}^2/\text{s}$ , the group with the lower ADC value had worse DP compared to  
191 patients with the higher ADC value (80% and 20%, respectively, at 24 months). There  
192 was a similar tendency in the group with the higher  $\text{SUV}_{\text{max}} (\geq 7.9)$  to have a poor DP  
193 (60% and 40%, respectively, at 24 months). However, neither DP trend was statistically  
194 significant. ( $p = 0.09$ , and  $0.32$ , respectively).

195 As an exploratory analysis, a combination of ADC value and  $\text{SUV}_{\text{max}}$  with the  
196 same threshold values was investigated. When patients were divided into two groups  
197 (high-risk group: patients with ADC value  $\leq 1.05 \times 10^{-3} \text{mm}^2/\text{s}$  and  $\text{SUV}_{\text{max}} \geq 7.9$ ; and  
198 low-risk group: all other patients), the numbers of patients were well balanced between  
199 the groups (8 and 7 patients for the high- and low-risk groups, respectively). The high-risk  
200 group had significantly worse DP ( $p = 0.036$ ). The cumulative incidence rates of DP were  
201 75.0% (six patients) in the high-risk group and 28.6% (two patients) in the low-risk  
202 groups, respectively, at 24 months (Fig. 3). The two groups had a similar number of  
203 patients, and similar characteristics (Table 2).

204 The OS at 24 months was 50% (four patients died) in the high-risk group and 57%  
205 (three patients died) in the low-risk group. However, from the viewpoint of cancer specific

206 death, the survival rates were 60% (three patients died) in the high-risk group and 83%  
207 (one patient died) in the low-risk group. The cumulative incidence rates of LP at 24  
208 months were 14% (one patient) in both groups. The tumour diameter, pre-treatment ADC  
209 value and  $SUV_{max}$  of the patient in the high-risk group were 28 mm,  $1.04 \times 10^{-3} \text{ mm}^2/\text{s}$   
210 and 7.9. Those of the patient in the low-risk group were 42 mm,  $1.19 \times 10^{-3} \text{ mm}^2/\text{s}$  and  
211 13.6, respectively.

212

## 213 **Discussion**

214 To the best of our knowledge, this is the first study to evaluate the use of  
215 DW-MRI for predicting the clinical outcomes in NSCLC patients treated with SBRT. It is  
216 also the first direct comparison of FDG-PET and DW-MRI in terms of prognosis  
217 prediction for NSCLC patients who have undergone SBRT.

218 We found that patients presenting with stage I NSCLC and either a lower ADC  
219 value, or with a higher  $SUV_{max}$  tended to have a poor DP after SBRT although the  
220 difference was not statistically significant. The use of ADC value and  $SUV_{max}$  in  
221 combination was a better predictor for DP than either biological marker alone.

222 Several previous studies on PET in NSCLC patients treated with SBRT have been  
223 published. Various controversial results have been reported regarding the use of  
224 FDG-PET for prognosis. In a recent study of 152 patients treated with SBRT of 40 to 60  
225 Gy in five fractions,  $SUV_{max}$  was a significant predictor of OS, disease-free survival, and

226 LP [14], although this study included patients with pathologically unconfirmed NSCLC.  
227 Another analysis showed that pre-treatment  $SUV_{max}$  was a significant predictor for  
228 disease-free survival and distant failure in 82 patients [12]. Burdick et al. evaluated the  
229 pre-treatment  $SUV_{max}$  in 72 patients treated with SBRT with a median follow-up of 16.9  
230 months, however  $SUV_{max}$  did not predict OS and DP [15]. We found a correlation  
231 between  $SUV_{max}$  and DP, although there was no statistically significant correlation with  
232 DP.

233 The conventional PET scan has several problems for evaluation of  $SUV_{max}$ . First, the  
234 spatial resolution of the PET scanner is low. Second, the PET image is often blurred due  
235 to respiratory motion, especially in the lower lobes of the lung and upper abdominal  
236 organs.  $SUV_{max}$  is higher when measured using respiratory gating PET or CT  
237 reconstruction than when using conventional techniques in lung tumours [19]. If we had  
238 used the respiratory gating method in this study, a significant difference might have been  
239 observed.

240         The use of DW-MRI for predicting the therapeutic effect and prognosis is also  
241 controversial. To date, no published study has addressed DWI in early-stage NSCLC  
242 patients treated with SBRT. A few reports have discussed DW-MRI and lung cancer  
243 treated with chemoradiotherapy. Ohno et al. reported a correlation between DW-MRI and  
244 PET in a study of 64 patients with locally advanced NSCLC (stage III) treated with  
245 conventional chemoradiotherapy. They found that higher ADC and  $SUV_{max}$  values were

246 significantly associated with poor prognosis. OS and progression-free survival of the two  
247 groups split at an ADC value of  $2.1 \times 10^{-3} \text{ mm}^2/\text{s}$ , and a  $\text{SUV}_{\text{max}}$  of 10 showed a  
248 significant difference [20]. Several studies have suggested that the ADC value is a  
249 predictive factor for other organs. In a study that analysed 32 patients with  
250 hypopharyngeal or oropharyngeal squamous cell carcinoma who underwent pre-treatment  
251 DWI and definitive chemoradiotherapy, patients with a higher ADC value (more than  
252 median,  $0.79 \times 10^{-3} \text{ mm}^2/\text{s}$ ) had a significantly lower local control rate than patients with a  
253 lower ADC value [21]. In contrast, Micco et al. reported that lower average pre-treatment  
254 ADC values were associated with high-risk features such as International Federation of  
255 Gynaecology and Obstetrics (FIGO) stage and LN metastases [10]. In another study, a  
256 lower ADC value was associated with shorter cancer-specific survival in patients with  
257 upper urinary tract cancer treated only with surgery [11]. Our result of a lower ADC value  
258 being associated with a poor prognosis after SBRT is in agreement with the latter reports.  
259 Several factors may have caused the different results. First, these studies defined ADC  
260 value differently. Different measures may be used to define the ROI and evaluate the  
261 ADC values, for example, using a minimum ADC value, a mean ADC value, or  
262 histogram analysis, etc [22-24]. We used the mean ADC value and avoided the cystic and  
263 necrotic areas to not affect the ADC value of the tumour. Second, the cancer type, clinical  
264 stage, and treatment strategies were different between the studies.

265           Some negative correlations between ADC value and cell density have been  
266 observed in certain malignancies. Tumours with a lower ADC value are more likely to  
267 have viable proliferative cells, which are sensitive to chemotherapy and radiotherapy.  
268 Conversely, the presence of inflammatory changes, necrosis, and fibrosis influence ADC  
269 value, which is correlated with interstitial water content and low cell density in  
270 histological samples [25, 26]. The lower the ADC value, the more effective the  
271 chemotherapy and/or radiotherapy [10, 20, 27].

272           Tumour size, patient gender, and operability are other prognostic factors suggested  
273 for early stage NSCLC treated with SBRT [5, 28, 29]. Our results suggest that the  
274 functional imaging modalities such as DW-MRI and PET could be a good predictor of  
275 clinical outcomes.

276           A limitation of this study is that the sample size was small. We introduced internal  
277 fiducial markers to a part of lung cancer patients in October 2010 to improve tumour  
278 localization during SBRT. The fiducial markers were made of gold and were inserted into  
279 bronchiole near the tumour [30]. Then, we stopped patient enrolment into the present  
280 study because of a concern that the gold markers might spoil image quality of DW-MRI.  
281 Despite of the small number, the present study indicated pre-treatment DW-MRI could be  
282 a predictor for clinical outcomes. A future study is warranted to prospectively evaluate the  
283 additional role of DW-MRI to FDG-PET before lung SBRT.

284           The present study did not evaluate ADC values after SBRT. There are some  
285 studies investigating the use of DW-MRI for predicting therapeutic effect of  
286 chemoradiation by comparing ADC values before and after treatment. Liu et al reported  
287 the percentage ADC value change after 1 month correlated positively with size reduction  
288 after 2 months of chemoradiation in 17 patients with cervical cancer [27]. Another study  
289 reported the ADC value at the time of 20 Gy was significantly higher in responders  
290 compared to non-responders in 27 patients with primary clinical T4 oesophageal  
291 carcinoma treated with chemoradiation [31]. We are planning a study to evaluate  
292 usefulness of DW-MRI in evaluation of the tumour response after SBRT and in  
293 distinction of treatment-related change from recurrence.

294 The consideration of more intensive therapy to prevent disease progression especially in  
295 high-risk patient is warranted. For example, dose escalation such as peripheral dose  
296 prescription and heterogeneous distribution, or systemic chemotherapy. However, early  
297 stage NSCLC patients treated with SBRT are often elderly and cannot tolerate  
298 chemotherapy. Thus, dose escalation is considered an appropriate strategy.

299

### 300 **Conclusion**

301 A low ADC value on pre-treatment DW-MRI and higher  $SUV_{max}$  may be associated with  
302 DP in NSCLC patients after SBRT. The combined use of ADC value and  $SUV_{max}$  is a  
303 better predictor for DP.

305 **References**

- 306 [1] Grutters JP, Kessels AG, Pijls-Johannesma M, De Ruyscher D, Joore MA, Lambin  
307 P. Comparison of the effectiveness of radiotherapy with photons, protons and  
308 carbon-ions for non-small cell lung cancer: a meta-analysis. *Radiother Oncol*  
309 2010;95(1):32-40.
- 310 [2] Onimaru R, Shirato H, Shimizu S, Kitamura K, Xu B, Fukumoto S, et al. Tolerance of  
311 organs at risk in small-volume, hypofractionated, image-guided radiotherapy for  
312 primary and metastatic lung cancers. *Int J Radiat Oncol Biol Phys*  
313 2003;56(1):126-35.
- 314 [3] Onishi H, Shirato H, Nagata Y, Hiraoka M, Fujino M, Gomi K, et al.  
315 Hypofractionated stereotactic radiotherapy (HypoFXSRT) for stage I non-small  
316 cell lung cancer: updated results of 257 patients in a Japanese multi-institutional  
317 study. *Journal of thoracic oncology : official publication of the International*  
318 *Association for the Study of Lung Cancer* 2007;2(7 Suppl 3):S94-100.
- 319 [4] Timmerman R, Paulus R, Galvin J, Michalski J, Straube W, Bradley J, et al.  
320 Stereotactic body radiation therapy for inoperable early stage lung cancer. *JAMA*  
321 2010;303(11):1070-6.
- 322 [5] Matsuo Y, Shibuya K, Nagata Y, Takayama K, Norihisa Y, Mizowaki T, et al.  
323 Prognostic factors in stereotactic body radiotherapy for non-small-cell lung cancer.  
324 *Int J Radiat Oncol Biol Phys* 2011;79(4):1104-11.
- 325 [6] Rezaei MK, Nolan NJ, Schwartz AM. Surgical pathology of lung cancer. *Seminars*  
326 *in respiratory and critical care medicine* 2013;34(6):770-86.
- 327 [7] Higashi K, Ueda Y, Arisaka Y, Sakuma T, Nambu Y, Oguchi M, et al. 18F-FDG  
328 uptake as a biologic prognostic factor for recurrence in patients with surgically  
329 resected non-small cell lung cancer. *Journal of nuclear medicine : official*  
330 *publication, Society of Nuclear Medicine* 2002;43(1):39-45.
- 331 [8] Sunaga N, Oriuchi N, Kaira K, Yanagitani N, Tomizawa Y, Hisada T, et al.  
332 Usefulness of FDG-PET for early prediction of the response to gefitinib in  
333 non-small cell lung cancer. *Lung Cancer* 2008;59(2):203-10.
- 334 [9] Weber WA, Petersen V, Schmidt B, Tyndale-Hines L, Link T, Peschel C, et al.  
335 Positron emission tomography in non-small-cell lung cancer: prediction of  
336 response to chemotherapy by quantitative assessment of glucose use. *J Clin Oncol*  
337 2003;21(14):2651-7.
- 338 [10] Micco M, Vargas HA, Burger IA, Kollmeier MA, Goldman DA, Park KJ, et al.  
339 Combined pre-treatment MRI and 18F-FDG PET/CT parameters as prognostic  
340 biomarkers in patients with cervical cancer. *European journal of radiology* 2014.

- 341 [11] Yoshida S, Kobayashi S, Koga F, Ishioka J, Ishii C, Tanaka H, et al. Apparent  
342 diffusion coefficient as a prognostic biomarker of upper urinary tract cancer: a  
343 preliminary report. *European radiology* 2013;23(8):2206-14.
- 344 [12] Clarke K, Taremi M, Dahele M, Freeman M, Fung S, Franks K, et al. Stereotactic  
345 body radiotherapy (SBRT) for non-small cell lung cancer (NSCLC): is FDG-PET  
346 a predictor of outcome? *Radiother Oncol* 2012;104(1):62-6.
- 347 [13] Hoopes DJ, Tann M, Fletcher JW, Forquer JA, Lin PF, Lo SS, et al. FDG-PET and  
348 stereotactic body radiotherapy (SBRT) for stage I non-small-cell lung cancer.  
349 *Lung Cancer* 2007;56(2):229-34.
- 350 [14] Takeda A, Sanuki N, Fujii H, Yokosuka N, Nishimura S, Aoki Y, et al. Maximum  
351 standardized uptake value on FDG-PET is a strong predictor of overall and  
352 disease-free survival for non-small-cell lung cancer patients after stereotactic body  
353 radiotherapy. *Journal of thoracic oncology : official publication of the*  
354 *International Association for the Study of Lung Cancer* 2014;9(1):65-73.
- 355 [15] Burdick MJ, Stephans KL, Reddy CA, Djemil T, Srinivas SM, Videtic GM.  
356 Maximum standardized uptake value from staging FDG-PET/CT does not predict  
357 treatment outcome for early-stage non-small-cell lung cancer treated with  
358 stereotactic body radiotherapy. *Int J Radiat Oncol Biol Phys* 2010;78(4):1033-9.
- 359 [16] Takayama K, Nagata Y, Negoro Y, Mizowaki T, Sakamoto T, Sakamoto M, et al.  
360 Treatment planning of stereotactic radiotherapy for solitary lung tumor. *Int J*  
361 *Radiat Oncol Biol Phys* 2005;61(5):1565-71.
- 362 [17] Huang K, Dahele M, Senan S, Guckenberger M, Rodrigues GB, Ward A, et al.  
363 Radiographic changes after lung stereotactic ablative radiotherapy (SABR)--can  
364 we distinguish recurrence from fibrosis? A systematic review of the literature.  
365 *Radiother Oncol* 2012;102(3):335-42.
- 366 [18] Team RdC. R: A Language and Environment for Statistical Computing. In: R  
367 Foundation for Statistical Computing, 2012
- 368 [19] van Elmpt W, Hamill J, Jones J, De Ruyscher D, Lambin P, Ollers M. Optimal  
369 gating compared to 3D and 4D PET reconstruction for characterization of lung  
370 tumours. *European journal of nuclear medicine and molecular imaging*  
371 2011;38(5):843-55.
- 372 [20] Ohno Y, Koyama H, Yoshikawa T, Matsumoto K, Aoyama N, Onishi Y, et al.  
373 Diffusion-weighted MRI versus 18F-FDG PET/CT: performance as predictors of  
374 tumor treatment response and patient survival in patients with non-small cell lung  
375 cancer receiving chemoradiotherapy. *AJR American journal of roentgenology*  
376 2012;198(1):75-82.
- 377 [21] Ohnishi K, Shioyama Y, Hatakenaka M, Nakamura K, Abe K, Yoshiura T, et al.  
378 Prediction of local failures with a combination of pretreatment tumor volume and  
379 apparent diffusion coefficient in patients treated with definitive radiotherapy for

- 380 hypopharyngeal or oropharyngeal squamous cell carcinoma. *Journal of radiation*  
381 *research* 2011;52(4):522-30.
- 382 [22] Heo SH, Shin SS, Kim JW, Lim HS, Jeong YY, Kang WD, et al. Pre-Treatment  
383 Diffusion-Weighted MR Imaging for Predicting Tumor Recurrence in Uterine  
384 Cervical Cancer Treated with Concurrent Chemoradiation: Value of Histogram  
385 Analysis of Apparent Diffusion Coefficients. *Korean journal of radiology : official*  
386 *journal of the Korean Radiological Society* 2013;14(4):616-25.
- 387 [23] Matoba M, Tonami H, Kondou T, Yokota H, Higashi K, Toga H, et al. Lung  
388 carcinoma: diffusion-weighted mr imaging--preliminary evaluation with apparent  
389 diffusion coefficient. *Radiology* 2007;243(2):570-7.
- 390 [24] Mori T, Nomori H, Ikeda K, Kawanaka K, Shiraishi S, Katahira K, et al.  
391 Diffusion-weighted magnetic resonance imaging for diagnosing malignant  
392 pulmonary nodules/masses: comparison with positron emission tomography.  
393 *Journal of thoracic oncology : official publication of the International Association*  
394 *for the Study of Lung Cancer* 2008;3(4):358-64.
- 395 [25] Manenti G, Di Roma M, Mancino S, Bartolucci DA, Palmieri G, Mastrangeli R, et al.  
396 Malignant renal neoplasms: correlation between ADC values and cellularity in  
397 diffusion weighted magnetic resonance imaging at 3 T. *La Radiologia medica*  
398 2008;113(2):199-213.
- 399 [26] Sugahara T, Korogi Y, Kochi M, Ikushima I, Shigematu Y, Hirai T, et al. Usefulness  
400 of diffusion-weighted MRI with echo-planar technique in the evaluation of  
401 cellularity in gliomas. *Journal of magnetic resonance imaging : JMRI*  
402 1999;9(1):53-60.
- 403 [27] Liu Y, Bai R, Sun H, Liu H, Zhao X, Li Y. Diffusion-weighted imaging in  
404 predicting and monitoring the response of uterine cervical cancer to combined  
405 chemoradiation. *Clinical radiology* 2009;64(11):1067-74.
- 406 [28] Baumann P, Nyman J, Hoyer M, Wennberg B, Gagliardi G, Lax I, et al. Outcome in  
407 a prospective phase II trial of medically inoperable stage I non-small-cell lung  
408 cancer patients treated with stereotactic body radiotherapy. *J Clin Oncol*  
409 2009;27(20):3290-6.
- 410 [29] Dunlap NE, Lerner JM, Read PW, Kozower BD, Lau CL, Sheng K, et al. Size  
411 matters: a comparison of T1 and T2 peripheral non-small-cell lung cancers treated  
412 with stereotactic body radiation therapy (SBRT). *The Journal of thoracic and*  
413 *cardiovascular surgery* 2010;140(3):583-9.
- 414 [30] Ueki N, Matsuo Y, Nakamura M, et al. Intra- and interfractional variations in  
415 geometric arrangement between lung tumours and implanted markers. *Radiother*  
416 *Oncol* 2014;110(3):523-8.
- 417 [31] Imanishi S, Shuto K, Aoyagi T, Kono T, Saito H, Matsubara H.  
418 Diffusion-weighted magnetic resonance imaging for predicting and detecting the

419 early response to chemoradiotherapy of advanced esophageal squamous cell  
420 carcinoma. Digestive surgery 2013;30(3):240-8.

Table 1. Patients' characteristics (n =15)

Sex (male/female)	11/4
Age (years), median (range)	80, (70–86)
Performance status 0/1	11/4
Operability	
Operable/Inoperable	7/8
Smoking status	
Never smoker/ex-smoker	2/13
Histology	
Adenocarcinoma/SCC/NSCLC nos	7/6/2
Size of tumour (mm), median (range)	30, (14–42)
T stage	
T1a/T1b/T2a	4/6/5
Location	
Peripheral/Central	9/6
RUL/RML/RLL/LUL/LLL	4/1/4/3/3
Prescribed dose	
48 Gy/56 Gy/60 Gy	5/4/6

Abbreviations: SCC = squamous cell carcinoma; NSCLC nos = non-small cell lung cancer, not otherwise specified; RUL = right upper lung; RML = right middle lung; RLL = right lower lung; LUL = left upper lung; LLL = left lower lung. T stage was revised according to the 7<sup>th</sup> edition of the TNM classification for lung cancer.

Table 2. Patients' characteristics in the high- and low-risk groups.

The high-risk group consisted of patients with an apparent diffusion coefficient (ADC) value  $\leq 1.05 \times 10^{-3} \text{ mm}^2/\text{s}$  and maximum standardised uptake values ( $\text{SUV}_{\text{max}}$ )  $\geq 7.9$ .

The other patients were in the low-risk group. The two groups were not different statistically.

	High-risk group (n = 8)	Low-risk group (n = 7)
Sex (male/female)	6/2	5/2
Age (years), median	72–86, 80	70–83, 80
Performance status 0/1	6/2	5/2
Operability		
Operable/Inoperable	4/4	3/4
Smoking status		
Never smoker/ex-smoker	0/8	2/5
Histology		
Adenocarcinoma/SCC/NSCLC nos	4/3/1	3/3/1
Size of tumour (mm), median (range)	28.5(17–35)	30(14–42)
T stage		
T1a/T1b/T2a	2/3/3	2/3/2
Prescribed dose		
48 Gy/56 Gy/60 Gy	3/2/3	2/2/3

Abbreviations: SCC = squamous cell carcinoma; NSCLC nos = non-small cell lung cancer, not otherwise specified. T stage was revised according to the 7<sup>th</sup> edition of the TNM classification for lung cancer.

## Figures

Fig. 1. Scatter plot of the apparent diffusion coefficient (ADC) value and maximum standardised uptake ( $SUV_{max}$ ). There was no statistical correlation between ADC value and  $SUV_{max}$  ( $r = 0.046$ ).

Fig. 2. Scatter plot of the apparent diffusion coefficient (ADC) value and tumour diameter (A) and maximum standardised uptake ( $SUV_{max}$ ) and tumour diameter (B). There was no statistical correlation ( $p=0.64$  and  $0.63$ , respectively).

Fig. 3. Cumulative incidence of disease progression (DP) according to apparent diffusion coefficient (ADC) value (A), maximum standardised uptake ( $SUV_{max}$ ) (B), and the combination of ADC value and  $SUV_{max}$  (C). The group with the lower ADC value and higher  $SUV_{max}$  tended to have worse prognosis, although this result was not significantly significant ( $p = 0.09$  and  $0.32$ , respectively). When applying an optimal cut-off value of the ADC and  $SUV_{max}$ , the lower ADC value and higher  $SUV_{max}$  group had a significantly poorer prognosis ( $p = 0.036$ ); the combination was a strong predictor for DP.

## Figures

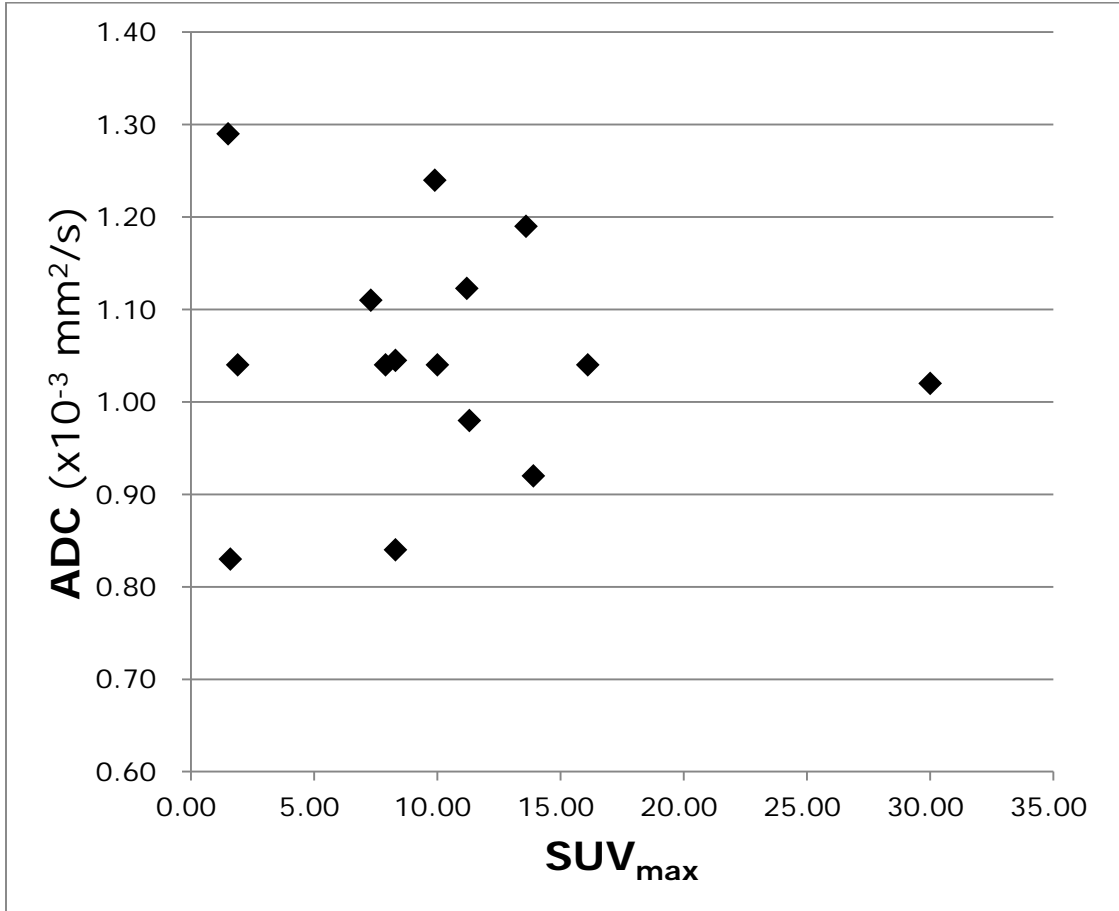
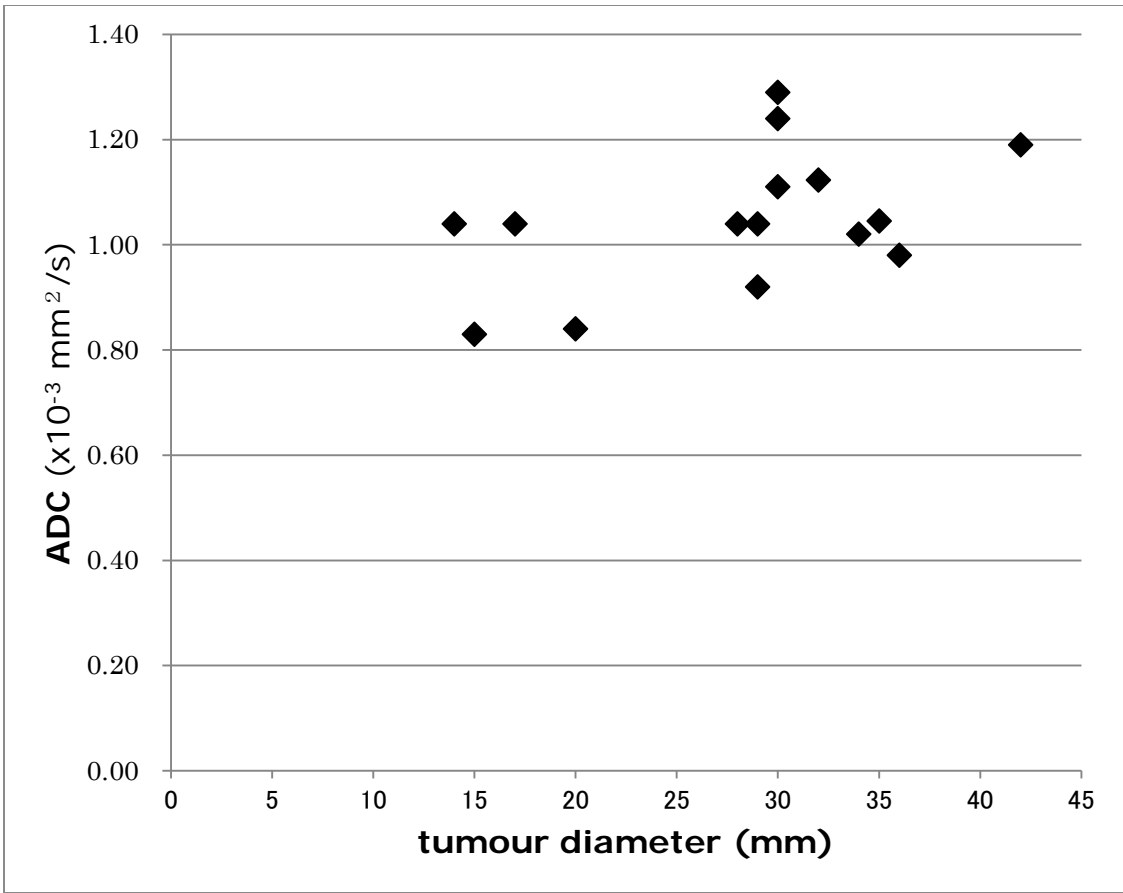


Fig. 1. Scatter plot of the apparent diffusion coefficient (ADC) value and maximum standardised uptake (SUV<sub>max</sub>). There was no statistical correlation between ADC value and SUV<sub>max</sub> ( $r = 0.046$ ).



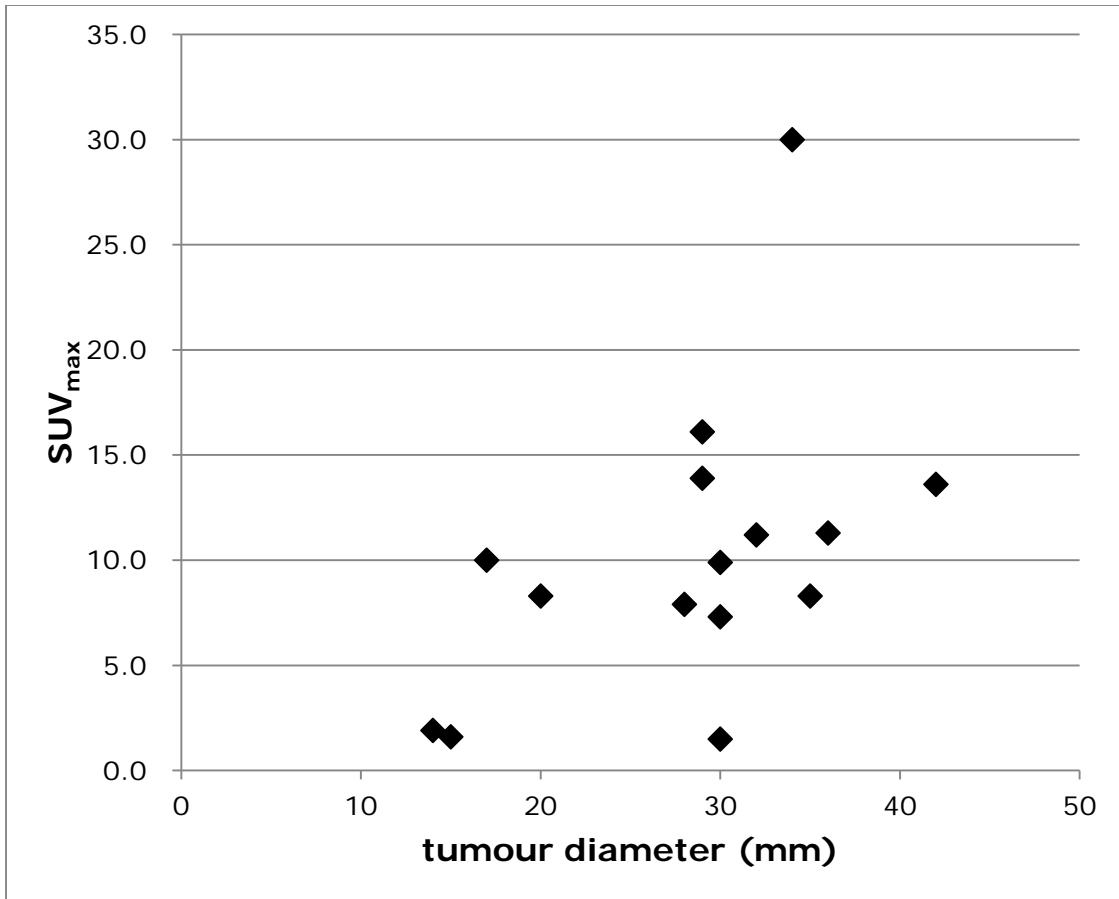
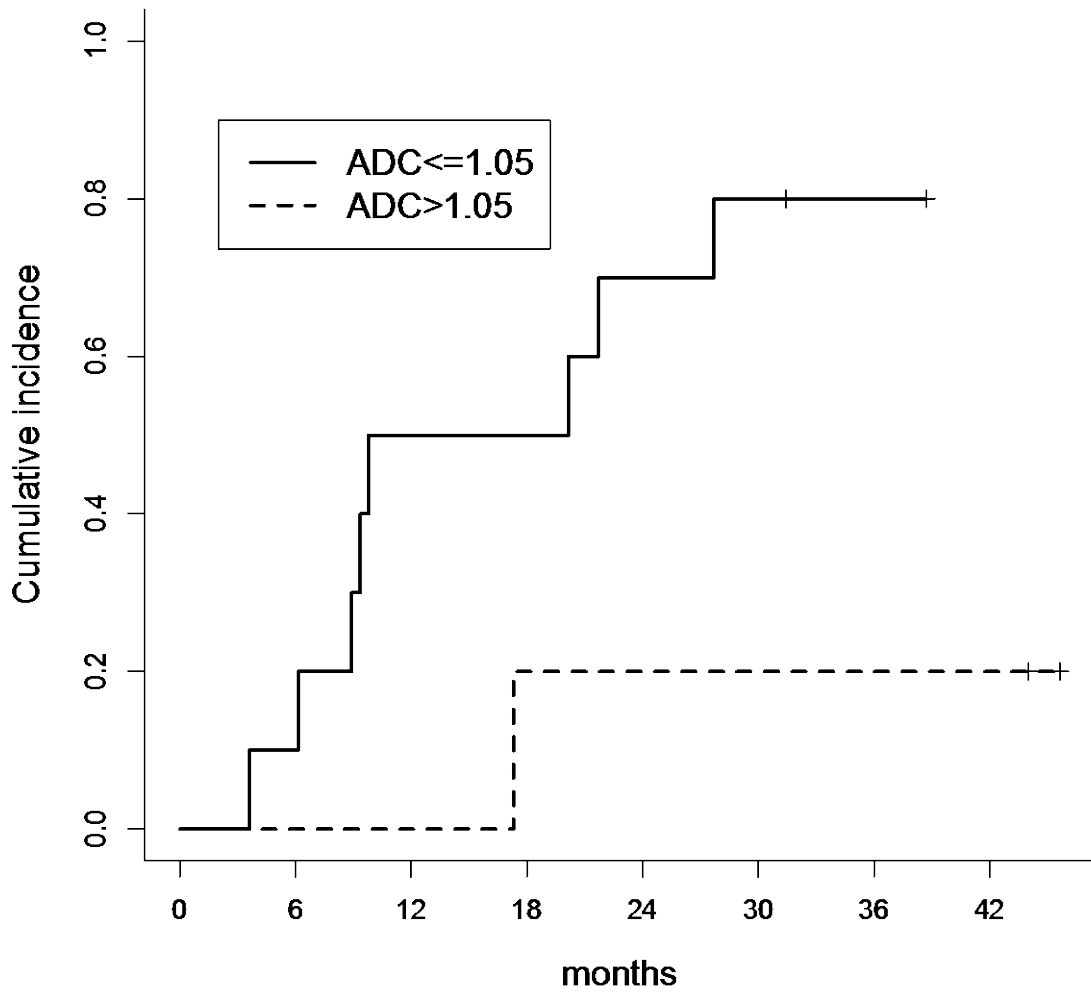


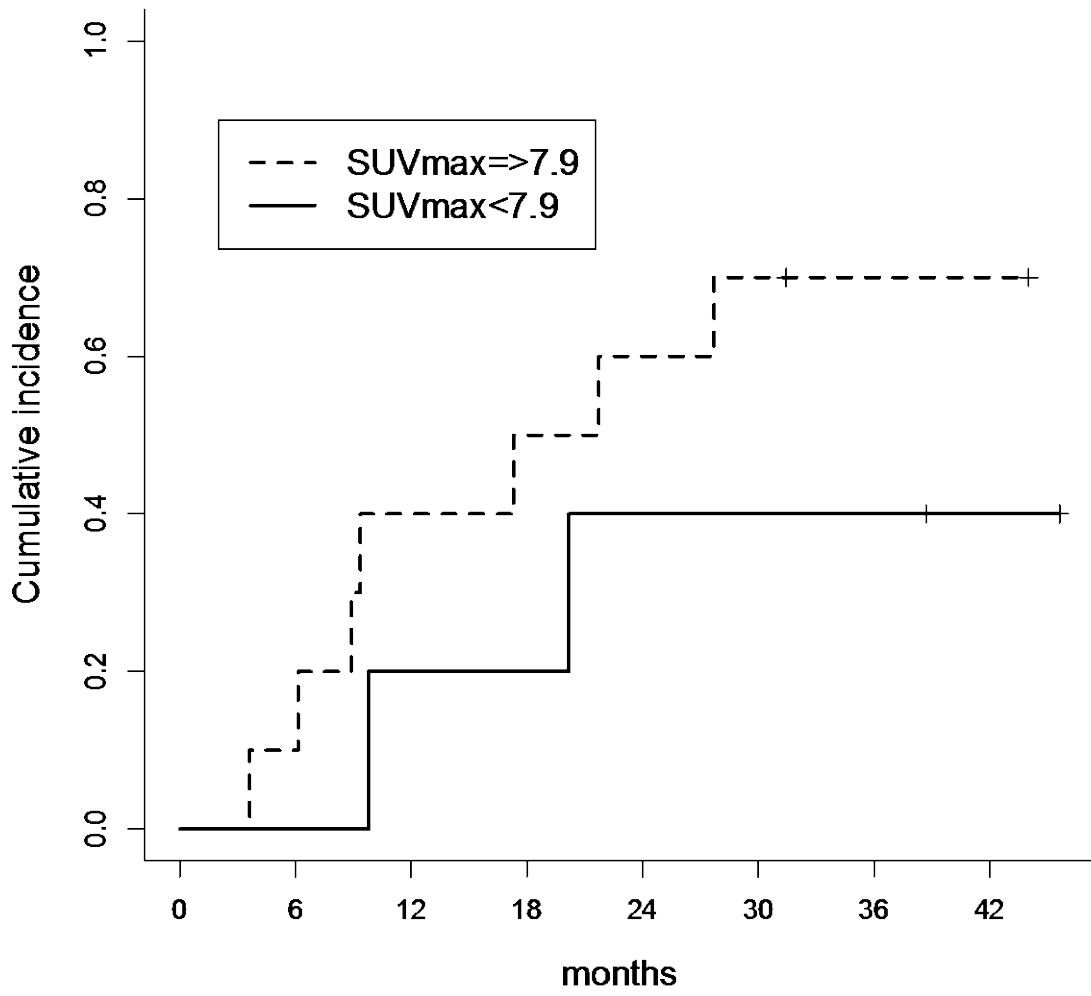
Fig. 2. Scatter plot of the (A) apparent diffusion coefficient (ADC) value and tumour diameter and (B) maximum standardised uptake (SUV<sub>max</sub>) and tumour diameter. There was no statistical correlation ( $p=0.64$  and  $0.63$ , respectively).

# Disease progression



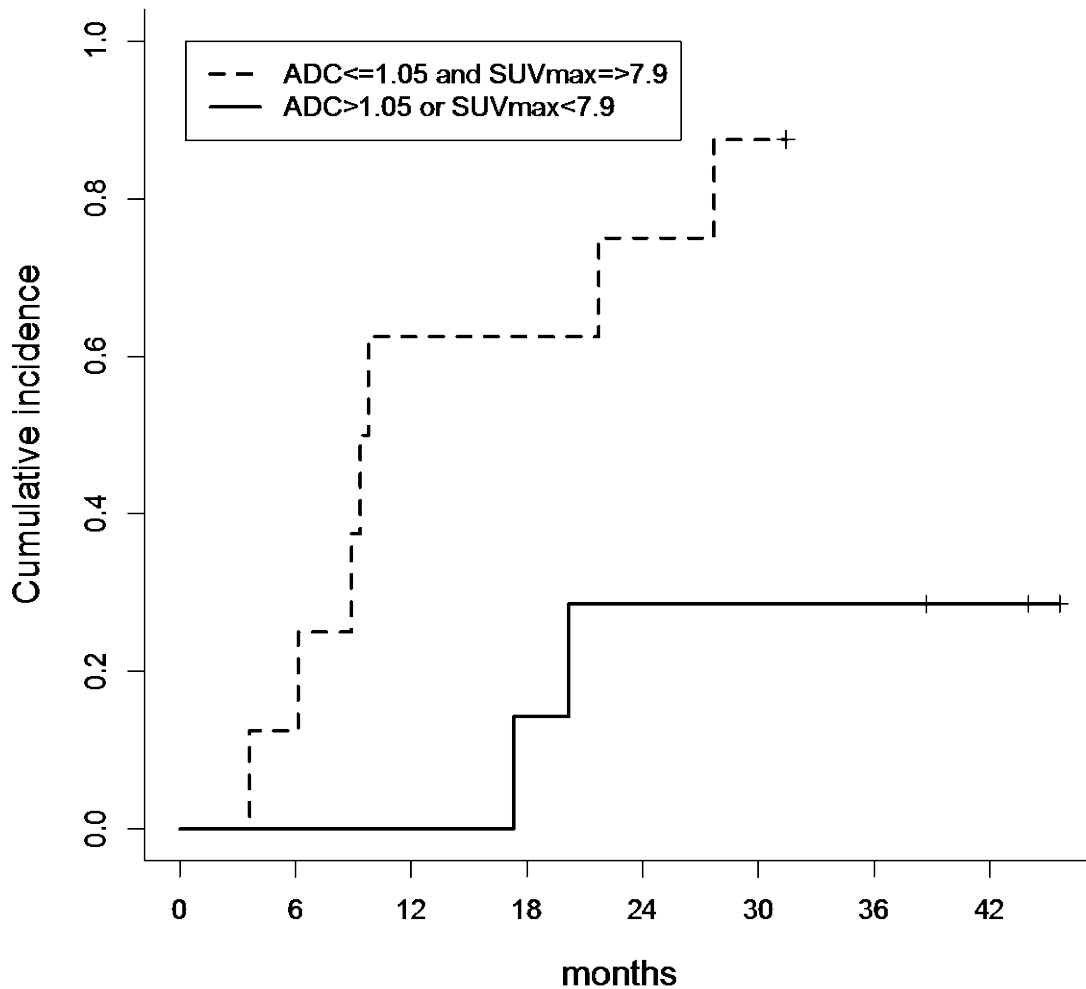
(A)

# Disease progression



(B)

## Disease progression



(C)

Fig. 3. Cumulative incidence of disease progression (DP) according to apparent diffusion coefficient (ADC) value (A), maximum standardised uptake ( $SUV_{max}$ ) (B), and the combination of ADC value and  $SUV_{max}$  (C). The group with the lower ADC value and higher  $SUV_{max}$  tended to have worse prognosis, although this result was not significantly significant ( $p = 0.09$  and  $0.32$ , respectively). When applying an optimal cut-off value of

the ADC and SUV<sub>max</sub>, the lower ADC value and higher SUV<sub>max</sub> group had a significantly poorer prognosis ( $p = 0.036$ ); the combination was a strong predictor for DP.